Global Journal of Researches in Engineering: A
Mechanical and Mechanics Engineering
Volume 14 Issue 3 Version 1.0 Year 2014
Type: Double Blind Peer Reviewed International Research Journal
Publisher: Global Journals Inc. (USA)
Online ISSN: 2249-4596 & Print ISSN: 0975-5861

Experimental Study and Verification of Wear for Glass Reinforced Polymer using ANSYS

By P. Prabhu, M. Suresh Kumar, Ajit Pal Singh & K. Siva
Defence University, Ethiopia

Abstract- The current design/manufacturing field looking for value added/engineering projects. In this study, an attempt has been aimed to predict the wear of the sliding surfaces in the development stage it self which will be results in the increase of durability of the components. The wear for a polymer-polymer sliding surface contact in dry condition can be obtained by creating simulation. There are two inputs required for determining the wear volume loss over its usage time. One is the nodal pressure value at the contact area for small sliding steps which can be calculated by subjecting the geometrical model to the finite element analysis. ANSYS was used as finite element tool. Another one is the friction coefficient which can be obtained by custom designed experiments. For the calculation of friction coefficient, prototype to be subjected to unlubricated pin-on-disc experimental setup. The wear rate can be calculated by graph by plotting between pressure and cycles. Swiveling of mirror over the base resulted in the wear. By the above techniques, the wear loss and reliability of the rear mirror can be predicted.

Keywords: glass reinforced polymer, wear, sliding contact, CATIA and ANSYS.

GJRE-A Classification : FOR Code: 291401

Strictly as per the compliance and regulations of:

Experimental Study and Verification of Wear for Glass Reinforced Polymer using ANSYS

P. Prabhu [α], M. Suresh Kumar [σ], Ajit Pal Singh [ρ] & K. Siva [ω]

Abstract- The current design/manufacturing field looking for value added/engineering projects. In this study, an attempt has been aimed to predict the wear of the sliding surfaces in the development stage it self which will be results in the increase of durability of the components. The wear for a polymer-polymer sliding surface contact in dry condition can be obtained by creating simulation. There are two inputs required for determining the wear volume loss over its usage time. One is the nodal pressure value at the contact area for small sliding steps which can be calculated by subjecting the geometrical model to the finite element analysis. ANSYS was used as finite element tool. Another one is the friction coefficient which can be obtained by custom designed experiments. For the calculation of friction coefficient, prototype to be subjected to unlubricated pin-on-disc experimental setup. The wear rate can be calculated by graph by plotting between pressure and cycles. Swiveling of mirror over the base resulted in the wear. By the above techniques, the wear loss and reliability of the rear mirror can be predicted.

Keywords: glass reinforced polymer, wear, sliding contact, CATIA and ANSYS.

I. Introduction

The interactions between two bodies that move in contact with each other manifest in friction and wear. Resulting in supplementary energy loss and failure of sliding elements, both processes have to be minimized. Since the application of a lubricating film between the contacting parts should be avoided for ecological reason or is impossible under certain working condition, polymers are increasingly used as self-lubricating materials in guidance, train boggies, bearings and ball-joints. The formation of a polymer transfer film onto the sliding counter face has beneficial effects on stable friction and low wear. However, the practical lifetime design of engineering polymers used under high loads and low sliding velocities can be troublesome, since most available data about their friction and wear properties are obtained from small-scale tests.

Author α: Research Scholar, Department of Engineering and Technology, Himalayan University, Arunachal Pradesh, India.
e-mail: lptprabhu@gmail.com
Author σ: Mechanical Engineering Department, Kings College of Engineering, Punalkulam, Thanjavur, India.
e-mail: sureshmech37@gmail.com
Author ρ: Production Engineering Department, College of Engineering, Defence University, Bishoftu, Ethiopia.
e-mail: singh_ajit_pal@hotmail.com
Author ω: Department of Mechanical Engineering, Hindustan College of Engineering and Technology, Coimbatore, Tamilnadu, India.
e-mail: sivri@rediffmail.com

In many cases, design engineers need specified tribological data to establish the performance of different available polymers for a given operational system in Archard's wear equation.

Experimental determination of life parameters in terms of wear has both cost and time impact. The ability to simulate wear and consequent useful life prediction can benefit product designers and manufacturers in multiple manners as, designing better products, contemplating better maintenance plans to avoid potential failures and avert financial losses. Some of the application areas where wear simulation can augment design are but not limited to: sliding or rotating components in automotives, engines and pumps, consumer products, prosthetic joints and lately MEMS (Microelectromechanical systems)-based micro machines. The finite element analysis-(FEA) based wear simulation and life prediction methodology presented in this research can be leveraged to any of the aforementioned areas.

a) Wear

Wear is the erosion of material from a solid surface by the action of another surface. It is related to surface interactions and more specifically the removal of material from a surface as a result of mechanical action.

b) Types of Wear

The study of the processes of wear is part of the discipline of tribology. The complex nature of wear has delayed its investigations and resulted in isolated studies towards specific wear mechanisms or processes. Some commonly referred to wear mechanism (or processes) include viz., adhesive wear, abrasive wear, surface wear, fretting wear, and erosive wear.

A number of different wear phenomena are also commonly encountered and represented in literature. Impact wear, cavitations wear, diffusive wear and corrosive wear are all such examples. These wear mechanisms; however, do not necessarily act independently in many applications. Wear mechanisms are not mutually exclusive. "Industrial wear" is the term used to describe the incidence of multiple wear mechanisms occurring in unison. Wear mechanisms and/or sub-mechanisms frequently overlap and occur in a synergistic manner, producing a greater rate of wear than the sum of the individual wear mechanisms.

c) Mechanism of Wear

Wear can be split into two majority categories: wear dominated by the mechanical behavior of materials and wear dominated by the chemical behavior of materials as shown in Table 1. Since finite element programs typically do not consider the chemical interactions between bodies or surfaces, these types of wear has not discussed in this paper. There are seven mechanical wear mechanisms listed (Table 1), however there are only three types of surface to surface interaction that can cause them: sliding (one surface sliding relative to another over long distances), fretting (one surface oscillates over minute distances relative to the other) and erosion (solid particles impinging on a single surface from an external source).

Table 1 : Classifications of wear mechanisms [6]

Classification	Wear mechanisms (Wear coefficient K range)
Wear dominated by mechanical behavior of materials	• Asperity deformation and removal (10^{-4}) • Wear caused by plowing (10^{-4}) • Delamination wear (10^{-4}) • Adhesive wear (10^{-4}) • Abrasive wear (10^{-2} to 10^{-1}) • Fretting wear (10^{-6} to 10^{-4}) • Wear by solid particle impingement
Wear dominated by chemical behavior of materials	• Solution wear • Oxidation wear • Diffusion wear • Wear by melting of the surface layer • Adhesive wear at high temperatures

For this study, only dry (non-lubricated) sliding wear has been considered. The actual wear mechanisms for dry sliding wear depends on a number of variables including viz., surface finish, surface geometry, orientation, sliding speed, relative hardness (of one surface relative to the other or relative to the abrasive particles between the surfaces), material microstructure and more. From these variables, it can be seen that wear rate is not a pure material property and does not always occur uniformly.

Finite element modeling of dry sliding wear can be accomplished one of two ways. First, the details of the surface interaction, including surface finish, can be included and calculated in the model. If that approach is taken, it would require that individual finite elements be removed from the model to simulate the gouging or plowing. This in turn requires that the size of the finite element be of the same size as the particles being removed since there are currently no options for removing part of an element (in ANSYS the element is either dead or alive).

As the particles being removed are on the size of molecules, the mesh density, at least near the wearing surface, would also need to be on the size of molecules. This is not a theoretical problem since finite elements are being used to analyze MEMS size devices but it is a practical problem since small size implies a large number of elements which requires large amounts of memory and disk space for the storage of the data generated by a finite element program.

The second approach would be to ignore the details of what is going on at the micro or nano scale and take a macro scale approach to the problem. On the macro scale, the size of the elements would be much larger than the anticipated changes due to wear and the calculations could be performed within the element rather than relying on the birth and death procedure needed at the surface level.

d) The Archard Equation

The starting point for any discussion of wear on the macro scale is the Archard equation (Podra and Andersson, 1999) [13], which states that:

$$W = K \times S \times P \qquad (1)$$

where, W is the worn volume, K is the wear per unit load per sliding distance and S is the sliding distance, P is the applied load.

Archard says "K may be described as the coefficient of wear and, in a series of experiments with the same combination of materials; changes in K denote changes in surface conditions". The Archard equation assumes that the wear rate is independent of apparent area of contact. However, it makes no assumptions about the surface topography (surface roughness effects are encompassed by the experimental wear coefficient) and it also makes no assumptions about variations with time. It must also be stated that although it is widely used, the Archard equation only provides for an order of magnitude estimate and is a true calculation of wear.

One of the more common methods for determining the value for K is to press a stationary pin using a preload of P into the surface of a rotating disk. The load P is known and the sliding distance S can be determined from the rotational speed of the disk and time that the disk has rotated. The amount of wear on the pin is determined by change in mass (weight) of the pin and the constant K calculated. This method for determining a constant wear coefficient for a given pair of surfaces has limitations. It ignores changes in apparent area of contact with time, also known as "running in" effects. It assumes that the direction of the load is constant which may not be the case in real conditions. And, it assumes that the surface topography of the experimental surfaces accurately represent the surfaces of interest.

Despite these limitations, it will be assumed that the values of wear coefficients determined by the pin-on-disk method or by other methods are accurate enough to use in engineering analysis. In engineering

applications, the loss of volume (and thus, loss of mass) may not be as important as the change of a given dimension at a given location on the device or structure. For example, we may be interested in the change of length of the pin in the pin-on-disk experiment. Or, we may be interested in the change of diameter for a radial bearing after a long period of time in use. The change of a single dimension can be calculated from the change in volume by dividing by the apparent area of contact assuming that the apparent area of contact is constant. When the contact area changes with time, a more sophisticated calculation must be performed to determine the change in desired dimension over time. This method for generating wear is not universally applicable.

First, it ignores the details of the surface and assumes that the full surface is in contact with the disk. This is similar to the usual assumption for contact in finite elements where the surface is assumed to be smooth. It also assumes that the direction of the load is constant and that the load is unchanging which may not be the case in real conditions. And if the state of stress at the surface is considered, the magnitude and direction of those surface stresses would also remain constant. A common type of wear is that generated by the repetitive application of a load on the same surface. The Archard equation would also imply that the particles would be removed from the surface in a uniform manner and that the surface would maintain the same general shape. That is that particles that exist in the valleys of the surface would be eroded at the same rate as particles at the peaks of the surface.

e) Stages of Wear

Under normal operating parameters, the property changes during usage normally occur in three different stages as follows:

- Primary or early stage or run-in period, where rate of change can be high.
- Secondary or mid-age process where a steady rate of aging process is maintained. Most of the useful or working life of the component is comprised in this stage.
- Tertiary or old-age stage, where a high rate of aging leads to rapid failure.

With increasing severity of environmental conditions such as higher temperatures, strain rates, stress and sliding velocities, the secondary stage is shortened and the primary stage tends to merge with the tertiary stage, thus drastically reducing the working life. Surface engineering processes are used to minimize wear and extend working life of material.

f) Study Approach

In this study, aim is to calculate the wear of the sliding contacts by using macro level approach. Equation (1) can be solved by using two parameters as inputs.

- Nodal pressure-it is the pressure at the crest of the projection areas, which can be obtained by FEA.
- Wear co-efficient can be calculated by using pin on disc experiment.
- Finding the life cycle of the component.

Above said approach to be followed to test the component shown in Figures 1 and 2.

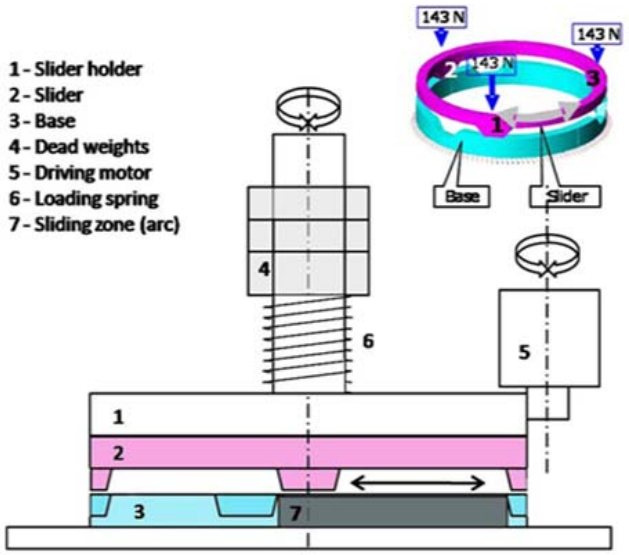

Figure 1 : Side rear view mirror in modern car in 2D

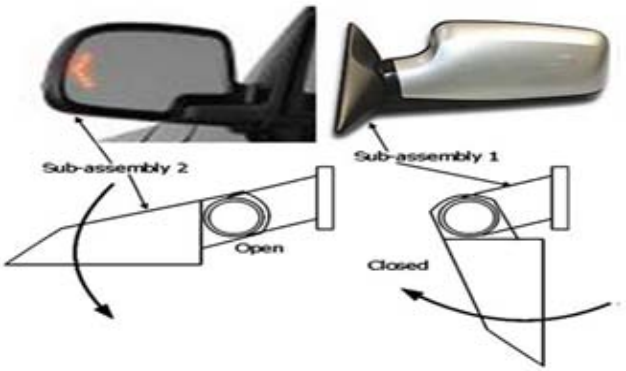

Figure 2 : Side rear view mirror in modern car

Swiveling of mirror over the base resulted in the wear. By the above techniques, the wear loss and reliability of the rear mirror can be predicted.

II. Literature Review

Podra and Andersson, (1999) [13] have studied the wear simulation approach with commercial finite element software ANSYS. A modeling and simulation procedure was proposed and used with the linear wear law and the Euler integration scheme. A spherical pin-on-disc unlubricated steel contact was analysed both

experimentally and with finite element method (FEM), and the Lim and Ashby wear map was used to identify the wear mechanism. It was shown that the FEA wear simulation results of a given geometry and loading can be treated on the basis of wear coefficient-sliding distance change equivalence. The finite element software ANSYS was well suited for the solving of contact problems as well as the wear simulation. The actual scatter of the wear coefficient was within the limits of 40-60% led to considerable deviation of wear simulation results. Due to the model simplifications and the real deviation of input data, the FEA wear simulation results was evaluated on a relative scale to compare different design options, rather than to be used to predict the absolute wear life.

Kim et al. (2005) [10] have proposed a numerical approach that simulates the progressive accumulation of wear in oscillating metal on metal contacts. The approach used a reciprocating pin-on-disk tribometer to measure a wear rate for the material pair of interest. This wear rate was an input to a FEA that simulates a block-on-ring experiment. After the simulation, two block-on-ring experiments were performed with the same materials that were studied in the reciprocating pin-on-disk experiments. The results from the FEA were in close agreement with the block-on-ring experimental results. This approach did not either rely on curve fitting or use the block-on-ring experimental data as model inputs. The FEA were performed by progressively changing nodal coordinates to simulate the removal of material that occurs during surface interaction. The continuous wear propagation was discretized and an extrapolation scheme was used to reduce computational costs of this simulation.

Zhang and Meng, (2006) [20] have proposed a linear sliding wear model with ratcheting effects to describe the wearing process and a simplified mathematical method was presented to simulate the wear of the rotor bushing sliding on the ground plane. The effects of geometry parameters, material properties and applied operating conditions on the evolution of dimensional and volumetric wear rates were explored for normally loaded rotating rotor bushing sliding on the ground plane. The hemispherical-bushing-on-ground-plane configuration finite element model was established and the implementation of the contact problem based on ANSYS finite element software and contact element approach was introduced to investigate contact problems in micro motors. Numerical simulations and results of the contact stresses and contact pressure were studied and the effects of wear coefficient, material selections, surface roughness and geometry structures, etc., were discussed in detail. It was indicated that the non-linear effects could not be ignored and these results must be evaluated on a relative scale to compare different design options.

Unal et al. (2004) [17] studied and explored the influence of test speed and load values on the friction and wear behavior of pure polytetrafluoroethylene (PTFE), glass fiber reinforced (GFR) and bronze and carbon (C) filled PTFE polymers. Friction and wear experiments were run under ambient conditions in a pin-on-disc arrangement. Tests were carried out at sliding speed of 0.32, 0.64, 0.96 and 1.28 m/s and under a nominal load of 5, 10, 20 and 30 N. The results showed that, for pure PTFE and its composites used in this investigated, the friction coefficient decrease with the increase in load. The maximum reductions in wear rate and friction coefficient were obtained by reinforced PTFE+17% glass fiber. The wear rate for pure PTFE was in the order of 10^{-7} mm^2/N, while the wear rate values for PTFE composites were in the order of 10^{-8} and 10^{-9} mm^2/N. Adding glass fiber, bronze and carbon fillers to PTFE were found effective in reducing the wear rate of the PTFE composite. In addition, for the range of load and speeds used in this investigation, the wear rate showed very little sensitivity to test speed and large sensitivity to the applied load, particularly at high load values.

III. Materials and Method

For rear side view mirror in modern car is made of polymers. In these base and slider are mating parts, base is rigidly fixed and slider is flexible surface contact with base is as shown in Figure 3.

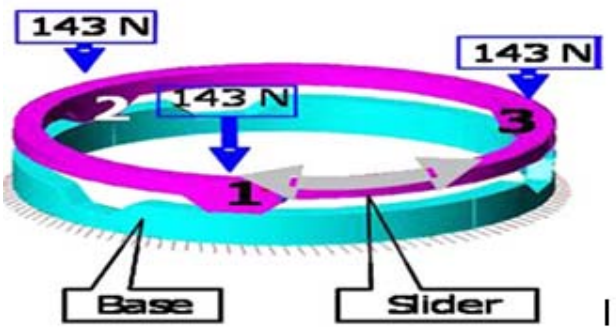

Figure 3 : Sliding contact at the swiveling joint

a) Existing Materials

The following materials (Tables 2 and 3) are used in existing model.

Table 2 : Properties of base material

Material	33% glass reinforced, heat stabilized black nylon copolymer resin
Density	1400 kgm^{-3}
Tensile strength	172 Mpa
Commercial name	Zytel 72G33HS1L by DuPont
Cost (INR)	210/Kg

Table 3 : Properties of slider material

Material	BK159, 45% glass reinforced modified polyethylene terephthalate
Density	1700 kgm^{-3}
Tensile strength	186 Mpa
Commercial name	Rynite 545 NC010 by DuPont
Cost (INR)	220/Kg

Coefficient of friction between 33% glass reinforced, heat stabilized black nylon copolymer resin and BK159, 45% glass reinforced modified polyethylene terephthalate=0.17 (as per previous experimentation set these values are obtained).

b) Selection of New Materials

In this study new materials were selected for the following reason:

- When the slider is in contact with base material the co-efficient of friction is high, due to this on the slider, the wear formation is high. Therefore changing the material of the slider will reduce the co-efficient and wear rate.
- When the wear formation is high automatically the life cycle of the component is reduced to low level. So in order to increase life cycle of the material. The new material was chosen is of 43% glass fiber reinforced polyamide 66 resin with high tensile strength, density, cost etc.

c) Proposed Materials

The following materials (Table 4) are used.

Table 4 : Properties of slider material

Material	43% glass fiber reinforced polyamide 66 resin.
Density	1490 kgm^{-3}
Tensile strength	236 Mpa
Commercial name	Zytel® 70G43L NC010
Cost (INR)	225/kg

d) Comparison of Materials

Table 5 compares the existing slider of BK159, 45% glass reinforced modified polyethylene terephthalate with 43% glass fiber reinforced polyamide 66 resin. Based on the comparison of proposed material with existing material, 43% glass fiber reinforced polyamide 66 resin properties is better than BK159, 45% glass reinforced modified polyethylene terephthalate, based on properties.

Table 5 : Comparisons of existing and new slider materials properties

Parts	Existing slider	New slider
Material	BK159, 45% glass reinforced modified polyethylene terephthalate	43% glass fiber reinforced polyamide 66 resin
Density	1700 kgm^{-3}	1490 kgm^{-3}
Tensile strength	186 Mpa	236 Mpa
Commercial name	Rynite 545 NC010	Zytel® 70G43L NC010
Cost (INR)	220/kg	225/kg

IV. Experimental Setup

The setup used in this study for the wear test is capable of creating reproducible sliding wear situation for accessing slide as shown in Figure 4. It consists of a pin on disc, loading panel and controller. The slide wears of slider and base polymer are carried out with different load by varying speed.

It determines the wear and co-efficient of friction of polymers under sliding contact. The tester is operated with a pin positioned perpendicular to the flat circular disc. The test machine causes the disc specimen to revolve about the disc centre; the sliding path is a circle on the disc surface.

Figure 5 shows experimental setup in laboratory. It consists of a pin on disc, loading panel and controller.

A sample pin is made up of 33% glass reinforced, heat stabilized black nylon copolymer resin and disc is 43% glass fiber reinforced polyamide 66 resin as shown in Figure 6.

Base is used as the disc and the slider corresponds to pin when it is compared to conventional pin-on-disc method. Slider is mounted on a rotary pneumatic cylinder, which can be revolved in clock and anti-clock wise directions relative to the fixed base. It consists of three contact pairs. The angular stroke of the slider is 32.3° as defined by the operating range of the mechanism. Thus the linear sliding distance can be computed for wear volume loss calculations.

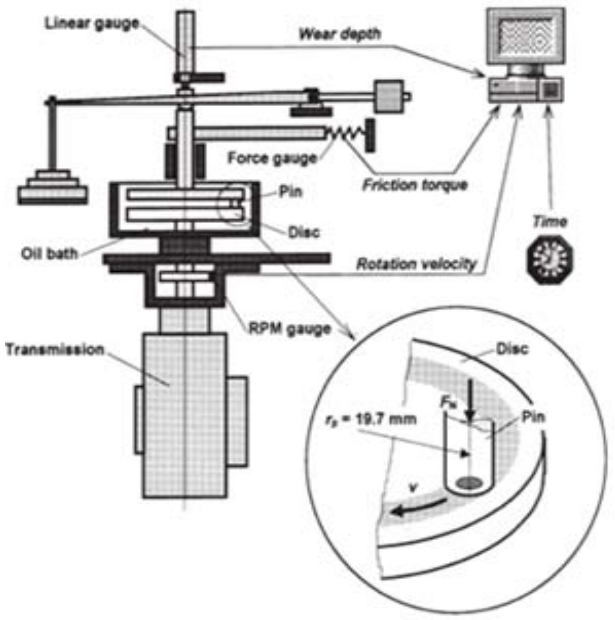

Figure 4 : Pin on disc setup

Figure 5 : Pin on disc experimental setup

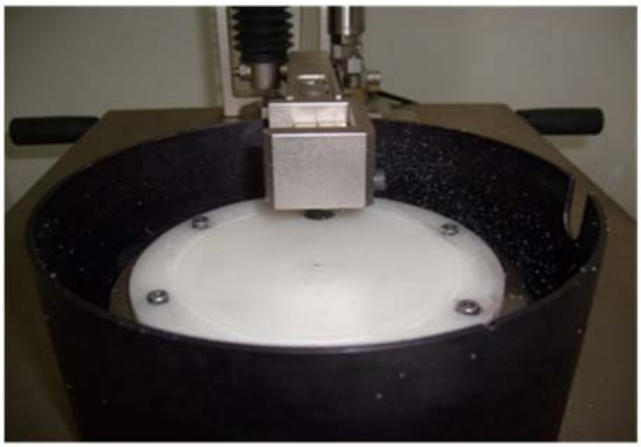

Figure 6 : Pin on disc arrangement

a) Readings

The graph (Figure 7) shows frictional force and wear from the pin on disk experiment.

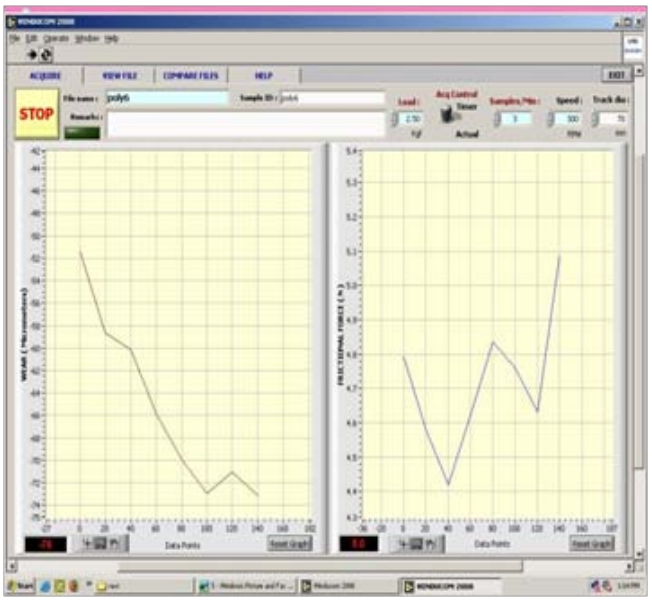

Figure 7 : Constant speed 300 rpm with varying loads

Tables 6 and 7 show the reading taken from the pin on disc experimental according to load and speed.

Table 6 : Under 300 rpm

Load (N)	Speed (RPM)	Time (S)	Wear (Microns)	Frictional force (N)
5	300	180	33	0.6
10	300	180	55	1.4
15	300	180	58	2.5
20	300	180	63	3.2
25	300	180	72	4.0
30	300	180	86	4.62

Table 7 : Under 400 rpm

Load (N)	Speed (RPM)	Time (S)	Wear (Microns)	Frictional force (N)
5	400	180	07	0.56
10	400	180	31	1.32
15	400	180	46	2.5
20	400	180	50	3.06
25	400	180	96	3.89
30	400	180	98	4.52

The graphs are plotted by pin on disc experimental setup according to load and speed (Tables 6 and 7).

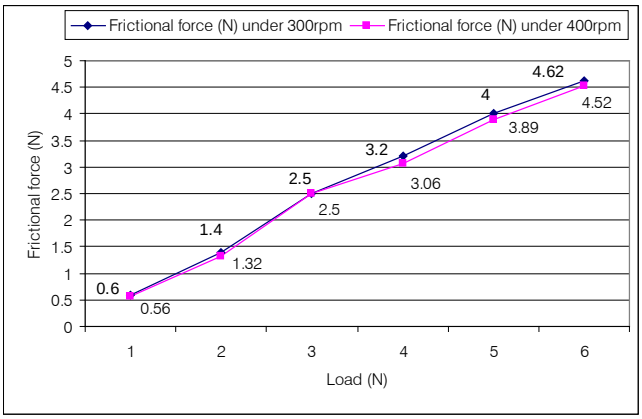

Figure 8 : Frictional force Vs Load (as per Tables 6 and 7)

The graph (Figure 8) reveals that when load is increasing corresponding frictional force is also increases. Based on Tables 6 and 7 data, the graph has plotted between load (N) and wear (microns) (Figure 9).

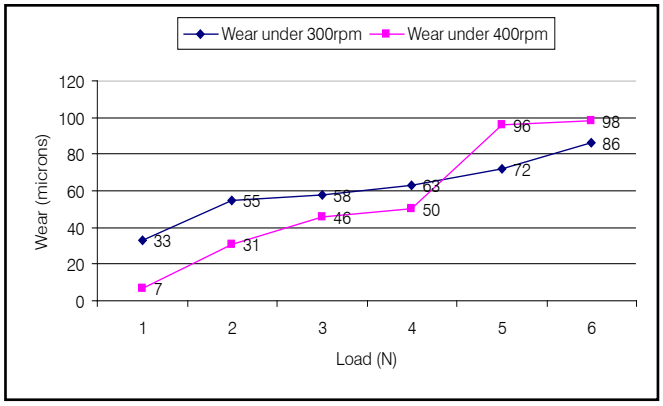

Figure 9 : Wear Vs Load (as per Tables 6 and 7)

The graph (Figure 9) reveals that when load is increasing corresponding wear is also increases. Wear calculated from experimental setup is as follows.

Co-efficient of friction = Frictional force ÷ Normal force Volumetric wear loss = 3.14 × (Radius of disc)^2 × Height of material lost = 3.14 × 6^2 × 0.695 = 78.562 mm^3

Tables 8 and 9 show the co-efficient of friction according to normal load and frictional force in 300rpm and 400rpm. Average co-efficient of friction between the 300 rpm and 400 rpm is 0.145. When compare this value with existing component co-efficient friction value is low. So this material is suitable for further process.

Average co-efficient of friction between the 300 rpm and 400 rpm is 0.145. When compare this value with existing component co-efficient friction value is low. So this material is suitable for further process.

Table 8 : Coefficient of friction under 300rpm

Normal load (N)	Frictional force(N)	Co-efficient of friction
5	0.6	0.12
10	1.4	0.14
15	2.5	0.166
20	3.2	0.16
25	4.0	0.16
30	4.62	0.154

Table 9 : Coefficient of friction under 400rpm

Normal load (N)	Frictional force(N)	Co-efficient of friction
5	0.56	0.112
10	1.32	0.132
15	2.5	0.166
20	3.06	0.153
25	3.89	0.155
30	4.52	0.150

V. Modeling and Analysis

a) Modeling

The modeling of slider and base was done by CATIA. It has three contact surfaces of slider with the base as shown in Figure 10. Figure 11 illustrates the CATIA model for one of the three detents depicted. To simplify the problem it is assumed that all three detents experience uniform and simultaneous wear. The problem is reduced to a two dimensional model with the assumption that wear would be uniform along the 3rd cartesian dimension (depth). In the Figure 11, slider and base are trapezoid and rectangle, respectively.

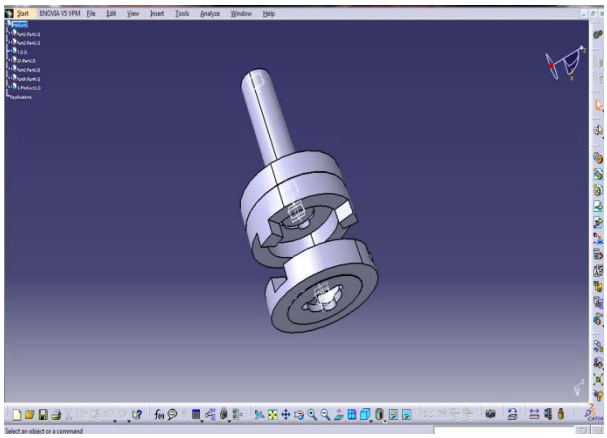

Figure 10 : Model of the component

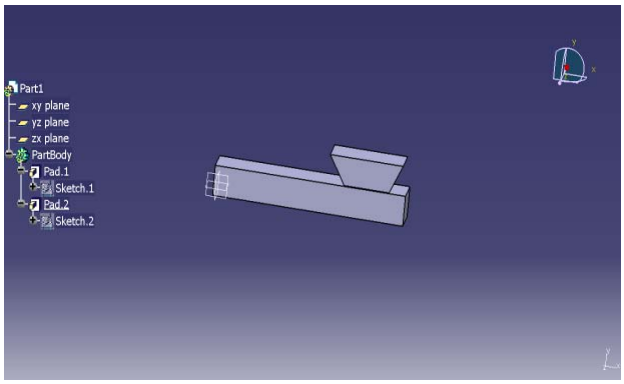

Figure 11 : Slider and base is trapezoid and rectangle model

b) General Contact Classifications

Contact problems fall into two general classes viz., rigid-to-flexible and flexible -to-flexible. In rigid-to-flexible contact problems, one or more of the contacting surfaces are treated as rigid (i.e., it has a much higher stiffness relative to the deformable body it contacts). In general, any time a soft material comes in contact with a hard material, the problem may be assumed to be rigid-to-flexible. Many metal forming problems fall into this category. The other class, flexible-to-flexible, is the more common type. In this case, both (or all) contacting bodies are deformable (i.e., have similar stiffness's).

c) Contact Problems

Contact problems are highly nonlinear and require significant computer resources to solve. It is important that you understand the physics of the problem and take the time to set up your model to run as efficiently as possible.

Contact problems present two significant difficulties. First, you generally do not know the regions of contact until you've run the problem. Depending on the loads, material, boundary conditions, and other factors, surfaces can come into and go out of contact with each other in a largely unpredictable and abrupt manner. Second, most contact problems need to account for friction. There are several friction laws and models to choose from, and all are nonlinear. Frictional response can be chaotic, making solution convergence difficult.

In addition to these two difficulties, many contact problems must also address multi-field effects, such as the conductance of heat and electrical currents in the areas of contact.

d) Nonlinear Analysis

If a structure experiences large deformations, its changing geometric configuration can cause the structure to respond nonlinearly. Nonlinear stress-strain relationships are a common cause of nonlinear structural behavior. Many factors can influence a material's stress-strain properties, including load history (as in elastoplastic response), environmental conditions (such as temperature), and the amount of time that a load is applied (as in creep response).

e) Surface-To-Surface Contact Elements

ANSYS supports both rigid-to-flexible and flexible-to-flexible surface-to-surface contact elements. These contact elements use a "target surface" and a "contact surface" to form a contact pair.

- The target surface is modeled with either TARGE169 or TARGE170 (for 2-D and 3-D, respectively).
- The contact surface is modeled with elements CONTA171, CONTA172, CONTA173, and CONTA174.

To create a contact pair, assign the same real constant number to both the target and contact elements. More details can be fined on defining these elements and their shared real constant sets in "surface-to-surface contact".

f) Steps in a Contact Analysis

The basic steps for performing a typical surface-to-surface contact analysis are listed. Each step is then explained in detail in the following sections.

- Create the model geometry and mesh.
- Identify the contact pairs.
- Designate contact and target surfaces.
- Define the target surface.
- Define the contact surface.
- Set the element KEYOPTS and real constants.
- Define/control the motion of the target surface (rigid-to-flexible only).
- Apply necessary boundary conditions.
- Define solution options and load steps.
- Solve the contact problem.
- Review the results.

g) Finite Element Method-Based Wear Simulation

So far none of the commercial FEA-based design and analysis software provides an integrated wear simulation tool. However, using the available contact analysis tools, indirect wear estimation approaches are proposed to estimate wear [13, 8]. Implementation of any such approach depends on the openness and the capability of FEA software to incorporate external algorithms. This section presents contact analysis in FEA and implementation of wear algorithm. Contact analysis in FEM is a nonlinear problem.

Contact stresses and contact pressures are the two main quantities sought in FEM-based wear simulation. The continuous and random dimensional change of wear surfaces poses a significant difficulty in sliding wear problems. Their shapes vary due to the sliding velocity, load, material parameters, and surface topographies, and will be changed as a result of the friction and wear. The important wear modeling task is the ability to obtain precise amount of worn material out of any sliding situation and for any geometry [7].

ANSYS, the commercial FEA software used for this research can handle several material and structural nonlinearities, i.e., plasticity, viscoelasticity, and friction. For contact problems, ANSYS can model contact condition with different types of contact element and present Lagrange multiplier, penalty function and direct constraint approaches. When meshing a model, the nodes on potential contacting surfaces comprise the layer of contact elements who's four Gauss integral points are used as contacting checkpoints [1].

h) Wear Simulation Algorithm

Contact analyses tools are used to solve sliding contact as a series of successive static load problems. After each sliding step nodal pressures at the contact nodes of the wearing member are extracted (recall the assumption made earlier that only softer of the two members would wear). The FEM based stepwise sliding wear calculation algorithm used in this research is presented.

Initially each node is moved individually, thus instigating the localized material removal. The distance moved by the contact node may not be uniformly distributed along the sliding surface. This not only leads to the prediction of height decays of the contact, but also indicates the approximate worn shape [13, 8].

However, after a few iterations, when the cumulative displacement of any contact node nears the element height, further movement of nodes destabilizes the FEA model. In this case a revised geometry of the worn contact has to be defined. The element height,

thus, mentioned depends on this choice of FEA software, meshing size, and element types used in the model.

i) Input Parameters

- Element types: Slider-Contact-CONTA171, base-target-TARGE169
- Force= 143N
- Co-efficient of friction=0.14
- Young's modulus=0.8E5
- Density: Slider=1490 kgm^{-3}, Base=1400 kgm^{-3}
- Possion ratio: 0.3

j) Finite Element Model

Figure 12 shows the component model in ANSYS which is imported from CATIA and illustrates the FE model for one of the three detents depicted. To simplify the problem it is assumed that all three detents experience uniform and simultaneous wear. The problem is reduced to a two dimensional model with the assumption that wear would be uniform along the 3rd Cartesian dimension (depth). In Figure 12, slider and base are trapezoid and rectangle, respectively.

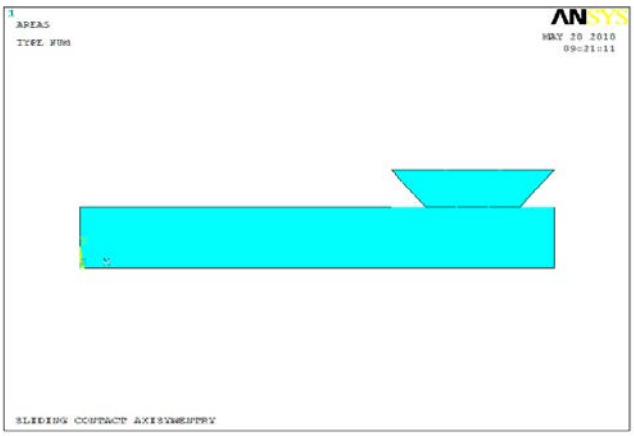

Figure 12 : Component model in ANSYS

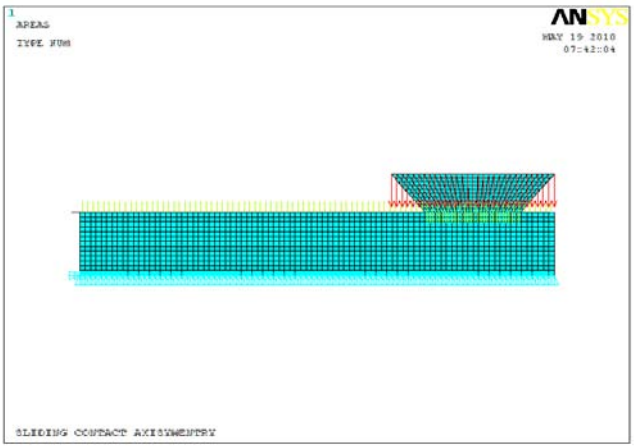

Figure 13 : It shows the finite element models in preprocessor stage

A uniform pressure is applied on top of the slider with displacement (sliding step) in x-axis. The sides of the base are constrained in all degrees of freedom to prevent rigid body motion. For the stability of surface-to-surface contact FEA model, it is mandatory that neither of the mating surfaces penetrate into each other. For this purpose ANSYS classifies the two surfaces as contact and target with specific element types assigned to each, namely CONTA171 and TARGE169.

Actual location of the contact depends on the geometry of the mating surfaces; ANSYS uses augmented Lagrangian formulation to find the contact regions. The model is limited to experience small deformations only. The structural equilibrium is found by incrementally changing the applied load. A converged solution is reached after a few Newton-Raphson iterations [1].

k) Sliding Step Size Determination

The model presented in Figure 14(a) is solved for different sizes of the sliding step. Internally each sliding step is divided into a number of sub-steps. The nodal pressure distribution for the contact nodes is plotted for each sub-step. It can be seen as the step size is increased the pressure distribution starts varying considerably. This behavior of FEA model affects the overall solution. Although a model solved with a smaller sliding step gives more accurate results, it comes at the expense of computational time. Therefore, the solution step is to be selected accordingly. In this case, the solution step of 0.1 mm was used.

l) Numerical Results

There are two key outcomes expected from an FEA wear analysis: height decay and worn geometry. Height decay over time gives an estimation of the component life, whereas the worn geometry gives an insight to the design's weak spots susceptible to wear.

Added to the above two factors, 'sliding contact wave propagation' over the sliding steps is also presented. To simulate the actual to and fro motion of the actual product, sliding distance was translated to repeated back and forward sliding strokes. The sliding stroke is FEA model illustrated in Figure 1 was solved for repeated sliding steps.

Due to the limited computational capability and development support from the FEA software used, we were not able to run the simulation for the complete number of sliding steps summing to the overall sliding distance of 400 meters. However, a reasonable accuracy was achieved with the assumption that the wear outcome remains unchanged for 100 successive sliding steps. At each 100 sliding step the cumulative height decay was incorporate in the FEA model and solved for next 100 steps.

m) Contact Pressure Analysis

Pressure distribution and contact status for the first sliding step solution for the contact problems are illustrated in Figures 14(a) and 14(b). It can be seen the pressure is distributed evenly at the middle region of the contact whereas the edges have maximum pressure concentration. This evidences that wear would be initiating from the contact edges. ANSYS classifies the contact status as 'near contact' and 'sliding', which are denoted by different color in Figure 14(a). Figure 14 (a) shows that the full face of the slider is in sliding contact. This initial contact will be converted to unevenly distribute small contact regions after few steps of wear as illustrated in the following results. Subsequent to the first contact solution step mentioned above, the contact is solved for the second sliding step by incorporated wear calculated from the above solution. This is indicative of wear on both edges that conform to the conclusion from the previous step, i.e., wear would be initiated from the edges of the sliding contact.

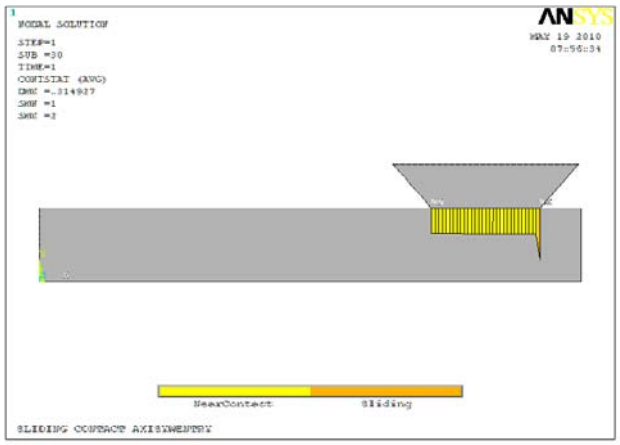

Figure 14 : (a) Contact status

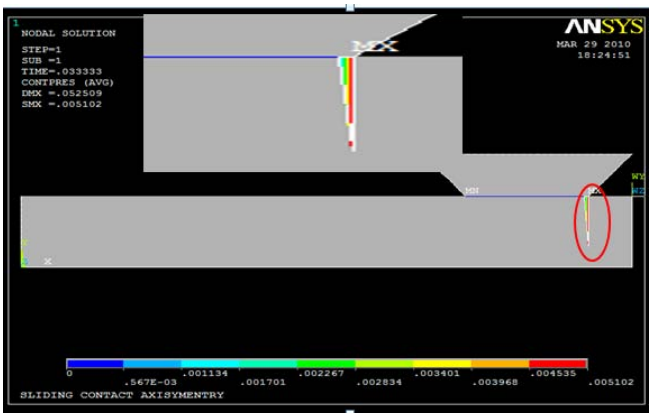

Figure 14 : (b) Pressure distribution

n) Contact Sliding Wave

Due to the elastic nature of polymers, the initially contacting surfaces do not maintain an absolute contact while sliding on top of each other The initially flat contact becomes a series of detachment waves also known as Schallamach waves moving along the contact zone during sliding [6, 13].

This phenomenon was observed during successive contact solutions. The oscillatory motion of the contact zone is now addressed. After incorporating first wear, the resulting contact is solved for the sliding step. Internal to the FEA software, each sliding step is divided into ten sub-steps. Analysis of the solution result at these sub-steps reveals the shifting of sliding contact zone along the face of the slider. This conforms to the wave phenomenon described above.

Using the ANSYS classification of contact status, we find that Figure 15 indicates the traveling of the actual contact zone along the face of the slider. Referring to Figure 14(b), the vertical line on the right indicates the starting datum for x-axis motion of the slider. A localized pressure distribution with the shape of two conjoined triangles for each sub-step indicates a very small contact detachment not physically visible on the scale of the drawing.

A contact separation travel opposite to the direction of the sliding can be seen in successive sub-steps 1, 5 and 10. Since the above data was obtained after incorporating a few iterations of wear, the wave encounters a cavity, resulting from the material removal, causing a contact gap terminating the wave in step 5. In the wave can be seen to follow a cyclic pattern in sub-step groups of {5, 10, 15} and {20, 25, 30}.

o) ANSYS Results

Figures 16 and 17 show the FEA of nodal pressure and cumulative cycle for proposed materials. Graph analysis the component wear rate with number of cycles.

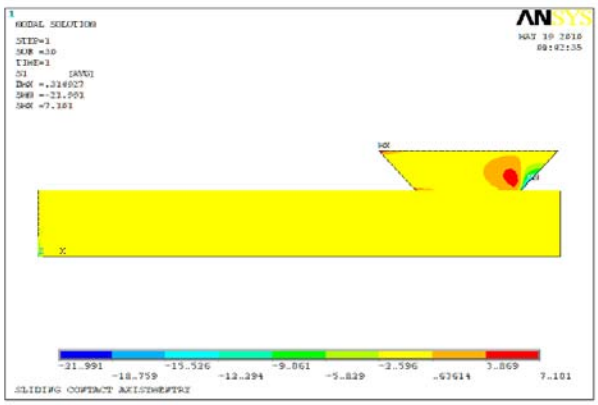

Figure 16 : Nodal pressures

The consolidated graph drawn by both experimental and ANSYS software readings is shown in Figure 17.

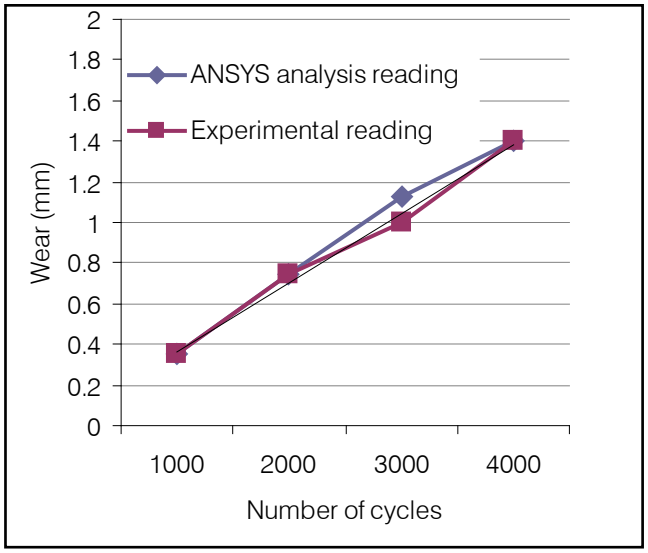

Figure 17 : Number of cumulative cycle for 0.314 mm

VI. Conclusion

For the slider material 43% glass fiber reinforced polyamide 66 resin gives the following results:

In ANSYS number of cycles=4016 for 1.4 mm

In experimental number of cycles=4100 for 1.4 mm

Nodal pressure=7.101N/mm^2

From the Figure 17 and result we concluded that contact analysis in ANSYS and experimentally pin on disc both of them, similar results are found which shows increasing in life cycle of the component by changing the material 43% glass fiber reinforced polyamide 66 resin for slider. The two important outcomes expected from a wear model from engineering standpoint are: change in dimensions and localized effects of wear. The FEA model presented addresses both aspects. Dimensional changes resulting from wear are seldom uniformly distributed; therefore any wear prediction model averages the changes in dimension across the contact in consideration. The FEA model can gives wear results at nodal level which can be averaged across the contact. The height decay results presented are obtained from averaging of nodal pressure. During the tests it was assumed that normal load is equally distributed to all three contacts.

References Références Referencias

1. ANSYS User's Manual for Version 10.0.
2. Ashraf, M. A., Najafabadi B. S., Gol O., Sugumar D. (2008) Time-to-failure prediction for a polymer–polymer swivelling joint. International Journal of Advanced Manufacturing Technology, 39(3-4): 271-278.
3. Ashraf, M. A., Najafabadi, B. S., Gol, O., Sugumar, D. (2007) Finite element analysis of a polymer-polymer sliding contact for Schallamach wave and wear. Key Engineering Materials, 348–349:633–636.
4. Ashraf, M.A., Najafabadi, B.S., Hsu, H.Y. (2006) Surface-surface contact wear prediction using FEA. In Research in Interactive Design, Springer, Paris.
5. Ashraf, M.A., Najafabadi, B.S., Hsu, H.Y. (2006) Wear prediction: A methodical approach. In Research in interactive design, Springer, Paris.
6. Bayer, R.G. (2002) Wear analysis for engineers. HNB Publishers, New York.
7. Cantizano, A., Carnicero, A., Zavarise, G. (2002) Numerical simulation of wear-mechanism maps. Computational Materials Science, 25:54-60.
8. Hegadekatte, V., Huber, N., Kraft, O. (2005) Finite element-based simulation of dry sliding wear. Modeling and Simulation in Materials Science and Engineering, 13 (1):57-75.
9. Hutchings, I.M. (1992) Tribology: friction and wear of engineering material. Edward Arnold Publishers, London.
10. Kim, N.H., Won, D., Burris, D., Holtkamp, B., Gessel, G.R., Swanson, P., Sawyer, W.G. (2005) Finite element analysis and experiments of metal/metal wear in oscillatory contacts. Wear, 258:1787–1793.
11. Lydersen, S., Rausand, M. (1987) A systematic approach to accelerated life testing. Reliab Eng 18(4):285–293.
12. Meng, H.C., Ludema, K.C. (1999) Wear models and predictive: Their form and content. Wear, 181-183:443-457.
13. Podra, P., Andersson, S. (1999) Simulating sliding wear with finite element method. Tribology International, 32:71-81.
14. Rabinowicz, E. (1995) Friction and wear of materials. Wiley, New York.
15. Sfantos, G.K., Aliabadi, M.H. (2007) Total hip arthroplasty wear simulation using the boundary element method. Journal of Biomechanics, 40: 378–389.
16. Taber Abrasion Test according to ISO 9352 OR ASTM D 1044.
17. Unal, H., Mimaroglu, A., Kadroglu, and Ekiz, H. (2004) Sliding Friction and Wear Behaviour of Polytetrafluoroethylene and its Composites under Dry Conditions. Material and Design, 25:239-245.
18. Williams, J.A. (2005) Wear and wear particles-Some fundamentals. Tribology International, 38(10): 863–870.
19. Zhang, W.M., Meng, G. (2006) Friction and wear study of the hemispherical rotor bushing in a variable capacitance micromotor. Microsystem Technologies, 12(4):283–292.
20. Zhang, W.M., Meng, G. (2006) Numerical simulation of sliding wear between the rotor bushing and ground plane in micromotors. Sensors and Actuators A: Physical, 126(1):15–24.

Global Journal of Researches in Engineering (A) Volume XIV Issue III Version I Year 2014
12

This page is intentionally left blank